

RNA-sequencing studies identify genes differentially regulated during inflammation-driven lung tumorigenesis and targeted by chemopreventive agents

Xuemin Qian¹ · Ali Khammanivong² · Jung Min Song¹ · Fitsum Teferi¹ · Pramod Upadhyaya¹ · Erin Dickerson^{1,2} · Fekadu Kassie^{1,2}

Received: 23 February 2015 / Accepted: 10 March 2015 / Published online: 21 March 2015
© Springer Basel 2015

Abstract

Introduction Chronic pulmonary inflammation has been consistently shown to increase the risk of lung cancer. Therefore, assessing the molecular links between the two diseases and identification of chemopreventive agents that inhibit inflammation-driven lung tumorigenesis is indispensable.

Materials and methods Female A/J mice were treated with the tobacco smoke carcinogen 4-(methylnitrosamino)-1-(3-pyridyl)-1-butanone (NNK) and lipopolysaccharide (LPS), a potent inflammatory agent and constituent of tobacco smoke, and maintained on control diet or diet supplemented with the chemopreventive agents indole-3-carbinol (I3C) and/or silibinin (Sil). At the end of the study, mice were sacrificed and tumors on the surface of the lung were counted and gene expression levels in lung tissues were determined by RNA sequencing.

Results The mean number of lung tumors induced by NNK and NNK + LPS was 5 and 15 tumors/mouse, respectively. Dietary supplementation with the combination of I3C and Sil significantly reduced the size and multiplicity (by 50 %) of NNK + LPS-induced lung tumors. Also, we found that 330, 2957, and 1143 genes were differentially regulated in mice treated with NNK, LPS, and NNK + LPS, respectively. The inflammatory response of lung tumors to LPS, as determined by the number of proinflammatory genes with altered gene expression or the level of alteration, was markedly less than that of normal lungs. Among 1143 genes differentially regulated in the NNK + LPS group, the expression of 162 genes and associated signaling pathways was significantly modulated by I3C and/or Sil + I3C. These genes include cytokines, chemokines, putative oncogenes and tumor suppressor genes and *Ros1*, *AREG*, *EREG*, *Cyp1a1*, *Arntl*, and *Npas2*.

Conclusion To our knowledge, this is the first report that provides insight into genes that are differentially expressed during inflammation-driven lung tumorigenesis and the modulation of these genes by chemopreventive agents.

Responsible Editor: Bernhard Gibbs.

X. Qian and A. Khammanivong contributed equally to this work.

Electronic supplementary material The online version of this article (doi:10.1007/s00011-015-0815-z) contains supplementary material, which is available to authorized users.

✉ Fekadu Kassie
kassi012@umn.edu

¹ Masonic Cancer Center, University of Minnesota, Mayo Mail Code 806, 420 Delaware Street SE, Minneapolis, MN 55455, USA

² College of Veterinary Medicine, University of Minnesota, Saint Paul, MN, USA

Keywords Lung tumors · Chemoprevention · 4-(methylnitro-samino)-1-(3-pyridyl)-1-butanone · Lipopolysaccharide · RNA sequencing

Abbreviations

NNK	4-(methylnitro-samino)-1-(3-pyridyl)-1-butanone
Sil	Silibinin
I3C	Indole-3-carbinol
RNA-Seq	RNA sequencing
LPS	Lipopolysaccharide

Introduction

Lung cancer is the leading cause of cancer death in the United States and worldwide [1]. Tobacco smoke, which contains 73 carcinogens, is recognized as the main cause of cancer [2, 3]. However, only about 10–15 % of smokers develop lung cancer in their life time [4]. It is not clear why some smokers develop lung cancer, while others do not. Epidemiological studies have consistently shown that smokers with COPD have a significantly increased risk for lung cancer compared with smokers without COPD [5, 6], which is one possible explanation for the variable susceptibility of smokers to lung cancer. Agents that contribute to the inflammatory effects of tobacco smoke include not only the many organic and inorganic chemicals in the gaseous, volatile, and particulate phases of cigarette smoke, but also tobacco-associated microbial elements such as bacteria, fungi, and diverse microbial toxins [7]. In particular, lipopolysaccharide (LPS), the major component of the cell wall of Gram-negative bacteria and a potent inflammatory agent, has been found in substantial amounts in the mainstream and sidestream cigarette smoke [8, 9]. Provocation of healthy volunteers with LPS has been used as a model of COPD as well as COPD exacerbation [10]. Similarly, studies in mouse models have shown that LPS-induced inflammatory and pathologic changes mimic changes observed in human subjects with COPD [11]. We have recently shown that repetitive administration of LPS to mice pre-treated with NNK significantly enhanced lung tumor multiplicity and tumor growth [12].

Although Rudolf Virchow noted, more than a century ago, the association between chronic inflammation and cancer [13], the underlying mechanisms are not yet fully known. Inflammatory signaling pathways and cytokines, reactive oxygen and nitrogen species, prostaglandins, and specific microRNAs are incriminated as potential links between chronic inflammation and cancer [14]. Further deciphering the molecular signatures of inflammation-driven tumorigenesis could lead to a better understanding of how the disease develops and the identification of novel diagnostic markers and preventive and therapeutic targets. A promising approach to achieve this goal is next-generation whole transcriptome RNA sequencing (RNA-Seq). Compared to microarrays, RNA-Seq has a larger dynamic range, the ability to detect all expressed transcripts as a function of depth of read coverage, the ability to detect transcript structure, and identify long noncoding RNAs that have important transcriptional and posttranslational gene regulatory roles [15].

In the present study, we have used RNA-Seq to characterize gene expression alterations associated with inflammation-driven lung tumorigenesis and modulation

of these effects by the chemopreventive agents silibinin (Sil) and/or indole-3-carbinol (I3C). Mice pre-treated with the tobacco smoke carcinogen 4-(methylnitrosamino)-1-(3-pyridyl)-1-butanone (NNK) received LPS, once a week, throughout the study and were maintained on a control diet or a diet supplemented with Sil and/or I3C. Sil is a constituent of the traditional medicinal plant milk thistle (*Silybum marianum*), whereas I3C is a derivative of glucobrassicin found in commonly consumed *Brassica* vegetables such as cabbage, cauliflower, broccoli, and Brussels sprouts. We have previously reported the strong antitumor activities of low doses of a combination of I3C and Sil in cell line and animal models of lung cancer [16].

Materials and methods

Chemicals, reagents and diets

I3C, Sil, and LPS were from Sigma (St Louis, MO). NNK was synthesized as described elsewhere [17]. Mouse diets AIN-93G/M were purchased from Harlan Teklad (Madison, WI).

Tumor bioassay

Female A/J mice, 5–6 weeks of age, were acquired from the Jackson Laboratory (Bar Harbor, ME). Mice were acclimated to the laboratory environment for 1 week in a pathogen-free environment. All experiments were performed according to the US National Institutes of Health (NIH) Guide for the Care and Use of Laboratory Animals, and approved by the Institutional Animal Care and Use Committee, the University of Minnesota.

The tumor bioassay was performed using a mouse model of inflammation-driven lung tumorigenesis as described previously [12]. Briefly, 1 week after arrival, mice were intraperitoneally treated with a single dose of NNK (100 mg/kg, in 0.1 ml physiological saline) or the vehicle alone. Beginning 1 week after NNK administration, groups of mice were intranasally instilled with LPS (5 µg/mouse in 50 µL of phosphate-buffered saline), once a week, until the end of the study. I3C (20 µmol/g diet) and Sil (20 µmol/g diet) were administered in the diet, individually or in combination. At week 22, the mice were euthanized with an overdose of carbon dioxide. The lungs were harvested and the tumors on the lung surface were counted and their sizes determined under a dissecting microscope. Lung tissues were preserved in RNA later solution (life technologies, Carlsbad, CA) and kept at –80 °C until used for RNA isolation.

RNA extraction

For mice treated with NNK, NNK + LPS, NNK + LPS + I3C, NNK + LPS + Sil and NNK + LPS + Sil + Sil, lung tumors (from three mice/group, 30 mg tumor tissue/mouse) were dissected, pooled, and used for the preparation of RNA. Histopathological studies of the tumors showed that all of the lung tumors were at adenoma stage. For mice treated with physiological saline solution (control group) or LPS, normal tissue was dissected (from three mice/group, 30 mg normal lung tissue/mouse) and used for the preparation of RNA. Total RNA was extracted from lung tumors or normal lung tissues using the miRNeasy Mini Kit (Qiagen, Valencia, CA) according to the manufacturer's instruction. The concentration (A260) and purity (A260/A280 and A260/A230) of RNA were determined using NanoDrop 1000 spectrophotometry. The integrity of the RNA preparations was confirmed by Agilent Bioanalyzer and/or Caliper GX. RNA samples with RNA integrity number higher than seven were selected for RNA sequencing.

Library preparation and RNA sequencing

Samples were prepared, using a TruSeq RNA Sample Preparation Kit (version 2), according to the manufacturer's instructions for RNA-Seq sample preparation. Twenty-one barcoded libraries (average gel size selected inserts of around 200 bp) were generated by University of Minnesota Biomedical Genomics Center Core Facility. The libraries were combined into three pools for sequencing (16 samples were sequenced in one lane and five samples were sequenced across two lanes using an Illumina's HiSeq 2000, 50 bp paired-end flow cell for 50 cycles). Twenty million reads were generated for each of the RNA samples. In the following step, a filter procedure was applied to remove sequences with low quality scores.

RNA-Seq data analysis

Paired-end RNA-sequencing data with mate-pair distance of 100 bp in FASTQ format were imported into CLC Bio Genomics Workbench 7 (CLC Bio, Qiagen, Boston, MA) for quality, mapping, and expression analyses. Sequencing quality analysis was performed using the built-in Sequencing QC Report within the Genomics Workbench to generate detailed reports of sequencing quality and over-represented sequences analyses. Transcriptomics analysis was then performed on samples that passed sequencing QC analysis to detect the expression level of each gene by mapping the sequencing reads to the latest mouse reference genome and annotation version mm10. Mapping was also performed on the inter-genic regions to identify potential

noncoding transcripts. Mapping options were set to the default settings, with read alignment mismatch cost = 2, insertion cost = 3, deletion cost = 3, length fraction = 0.8, similarity fraction = 0.8, auto-detect paired distances, strand specific = both, and maximum number of hits for a read = 10. An expression value for each gene was set to total exon counts (or total reads successfully mapped to one or more exons of each gene). Pair-wise empirical analysis of differential gene expression was performed on all pairs of sample groups using 'Exact Test' for two-group comparisons with trimmed mean of *M*-values (TMM) normalization to adjust for differences in sequencing depths [18], which is the same statistical algorithm implemented in EdgeR Bioconductor package [19]. False discovery rate (FDR)-corrected *p*-values of less than 0.05 and fold change of greater or equal to two were used as criteria for significantly regulated genes. Pathway analysis and gene ontology (Ingenuity Pathways Analysis; IPA, Ingenuity Systems, Inc., Redwood City, CA) were performed to identify putative diseases and functions associated with the differentially regulated genes. Genes of interest were validated by quantitative reverse transcriptase-polymerase chain reaction (qRT-PCR).

Quantitative RT-PCR analysis

RNA (1 µg) was reverse transcribed to cDNA in 20 µL reaction using the QuantiTect Reverse Transcription Kit (Qiagen, Valencia, CA) according to manufacturer's instructions. Quantification of mRNAs was performed on Applied Biosystems 7900HT Fast Real-Time PCR System with 384-Well Block Module (Life Technologies, Carlsbad, CA) using QuantiTect SYBR Green PCR Kit (Qiagen, Valencia, CA) and gene-specific forward and reverse primers (Supplemental Table S1). One microliter of the resulting cDNA sample was added to a 10 µL reaction and the final concentration of each primer is 0.5 µM. Samples were tested in triplicates and no template controls were included in each set of reactions. Amplification was carried out using the following conditions: 95 °C for 15 min, followed by 40 cycles of 94 °C for 15 s, 55 °C for 30 s, and 70 °C for 34 s. Melt curve analysis was performed at the end of every qPCR run. All samples were normalized to an internal control gene, Actb (β-actin), and the comparative Ct method was used to assess the relative gene expression.

Results

Differential gene expression analysis by RNA-Seq

The mouse tumor bioassay has clearly demonstrated that LPS-induced chronic pulmonary inflammation enhanced

Table 1 Effects of I3C and Sil, alone and in combination, against NNK-induced and LPS-enhanced lung tumors in A/J mice

Treatment group	Chemopreventive agent	Mice number initially/at termination	Lung tumors/mouse
None	None	10/10	0.1 ± 0.3
LPS	None	10/10	0.1 ± 0.2
NNK	None	15/15	4.8 ± 3.8
NNK + LPS	None	20/17	14.7 ± 4.1
NNK + LPS	I3C	20/20	15.0 ± 11.1
NNK + LPS	Sil	20/18	12.5 ± 5.2
NNK + LPS	I3C + Sil	20/20	7.1 ± 4.5 ^a

Beginning at age 6–7 weeks, groups of female A/J mice received NNK (100 mg/kg) by intraperitoneal injection. LPS was administered, once a week, by intranasal instillation (2 µg/mouse in 50 µl physiological saline solution, 25 µl in each nostril) throughout the study. I3C and Sil were given in the diet at a concentration of 20 µmol/g beginning 2 weeks after NNK administration until the termination of the study

^a Significant compared with group 1 ($p < 0.05$)

lung tumorigenesis, whereas dietary administration of I3C + Sil reduced the tumor burden (Table 1). Classification of the lung tumors into different size categories also revealed that the frequency of the largest tumors (>1 mm) was significantly reduced by Sil + I3C or I3C alone (from 6.3 ± 2.9 tumors/mouse in the control group to 1.0 ± 1.3 and 1.6 ± 1.8 tumors/mouse in mice given Sil + I3C or I3C alone, respectively, data not shown).

To characterize gene expression alterations associated with inflammation-driven lung tumorigenesis and to examine if these effects could be modulated by the chemopreventive agents Sil and/or I3C, total RNA was extracted from the lung tumors and the samples were processed for gene expression analysis by RNA-Seq. Total sequencing reads were achieved within at least 90 % of the targeted 20 million read depth for each sample, except for one control sample with a depth of 16.7 million reads. The sequencing depths for the rest of the samples ranged from 18.6 to 31.4 million reads. The calculated sequencing quality score was approximately 37.9 ± 0.37 (mean ± SD) across all samples, indicating that virtually all of the reads had zero errors and ambiguities (a score of 30 is considered a benchmark for quality in next-generation sequencing). To identify alterations in gene expression, the different treatment groups (NNK, LPS, NNK + LPS, NNK + LPS + Sil, NNK + LPS + I3C, and NNK + LPS + Sil + I3C) were compared to the vehicle control group. Based on gene expression profiles, an unsupervised principal component analysis (PCA) of covariance was first performed across all treatment groups. Both control and LPS groups showed distinct clusters directed toward opposite vectors (Fig. 1a), indicating strong intragroup

Fig. 1 Analysis of genes differentially expressed in lung tissues of mice treated with LPS, NNK, or NNK + LPS. **a** Principle component analysis of covariance among samples. **b** Venn diagram of differentially regulated genes. **c** Enriched canonical pathways of the differentially expressed genes using ingenuity pathway analysis (IPA). **d** IPA upstream regulator analysis. Positive z -score indicates activation (*red*) and negative z -score indicates inhibition (*green*). The magnitude of the z -score represents of the level of significance in prediction. Top upstream regulators are shown with a z -score of >2.5 or <-2.5 (color figure online)

correlation of gene expression but differences in intergroup gene signatures. Samples from NNK-treated mice not only clustered together but they were also closer to the groups treated with NNK + LPS and NNK + LPS + Sil, suggesting a transcriptomic signature different from the control- and LPS-treated groups. The transcriptomic signatures of the NNK + LPS + I3C- and NNK + LPS + Sil + I3C-treated groups were very similar, and their signatures were readily discerned from those of the other sample groups.

We next performed pair-wise Exact Test comparisons, with TMM normalization, to identify genes differentially expressed in each treatment group as compared to the vehicle control group. Based on our statistical significance criteria of FDR < 0.05 and fold change ≥ 2 or ≤ -2 , we identified 330 genes (240 upregulated and 90 downregulated) that were significantly deregulated in mice treated with NNK as compared to the control group (Fig. 1b; Supplementary Table S2). The most upregulated gene was *Spag11b* (216-fold), whereas *Cyp1a1* was the most downregulated gene (15-fold). The group treated with LPS alone showed the highest number of deregulated genes (a total of 2957 genes, 1761 genes upregulated and 1196 genes downregulated, Fig. 1b, Supplementary Table S3). As expected, the most upregulated genes were cytokines and chemokines (*Csf3*, *Ccl4*, *Cxcl9*, and *Il17A* increased 1794-, 378-, 951-, and 309-fold, respectively, compared to the control group), whereas *Ucp1* was the most downregulated gene (decreased 74-fold). Animals exposed to a combination of NNK + LPS showed 1143 deregulated genes (711 upregulated and 432 downregulated, Fig. 1b, Supplementary Table S4). Of these genes, 84, 647, and 183 genes overlapped with NNK, LPS, and both NNK- and LPS-treated groups, respectively, whereas 229 genes were uniquely deregulated. In this group, the most upregulated and downregulated genes, respectively, were *Spag11b* (826-fold) and *Slc28a1* (91-fold).

Genes associated with inflammation and immune responses were underrepresented in lung tissues of NNK + LPS-treated mice

According to the results from ingenuity pathway analysis (IPA), genes associated with inflammatory and immune

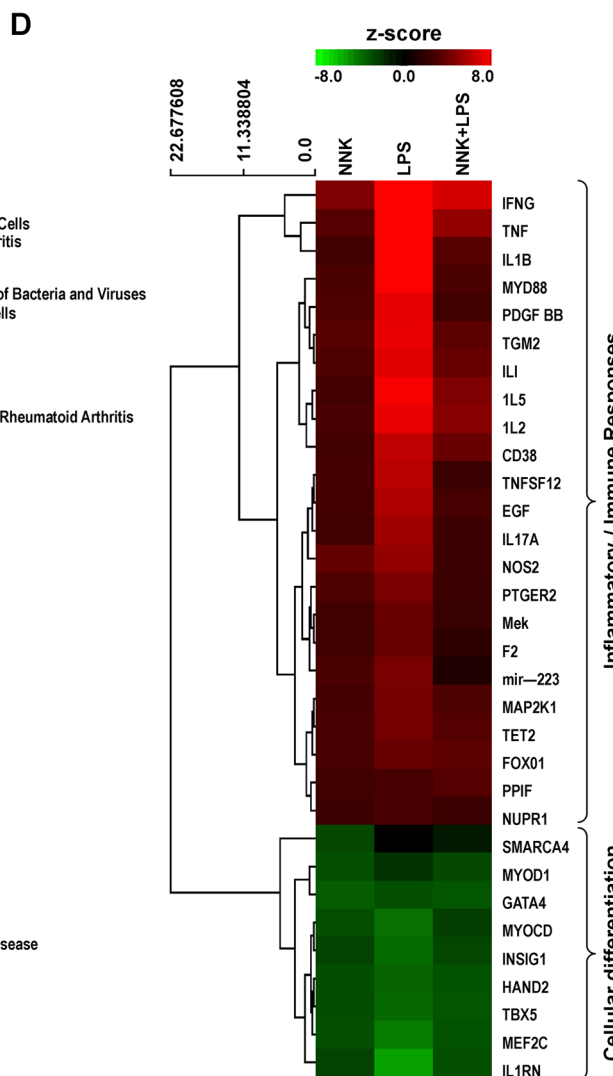
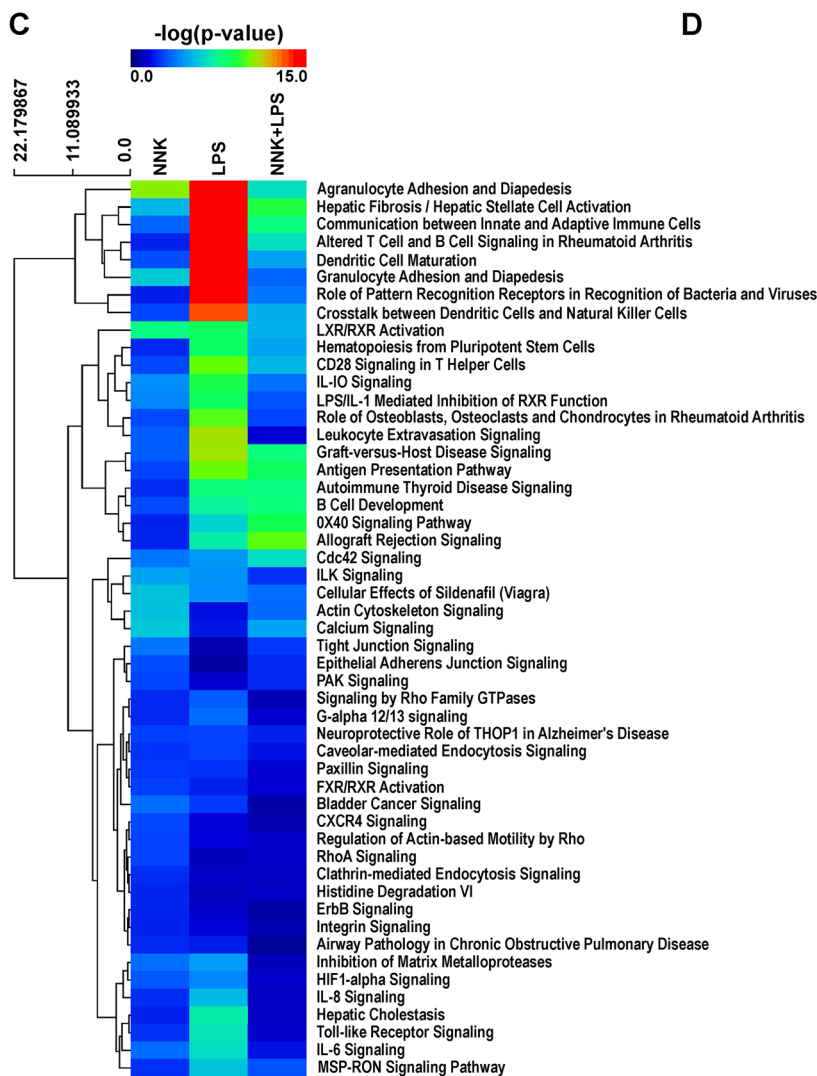
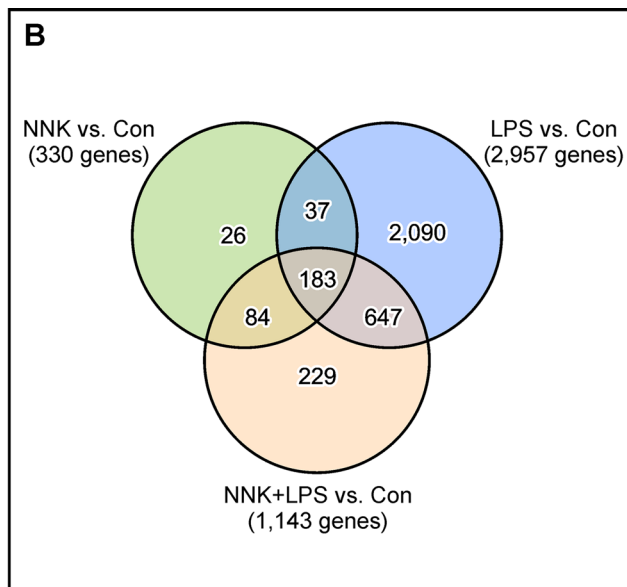
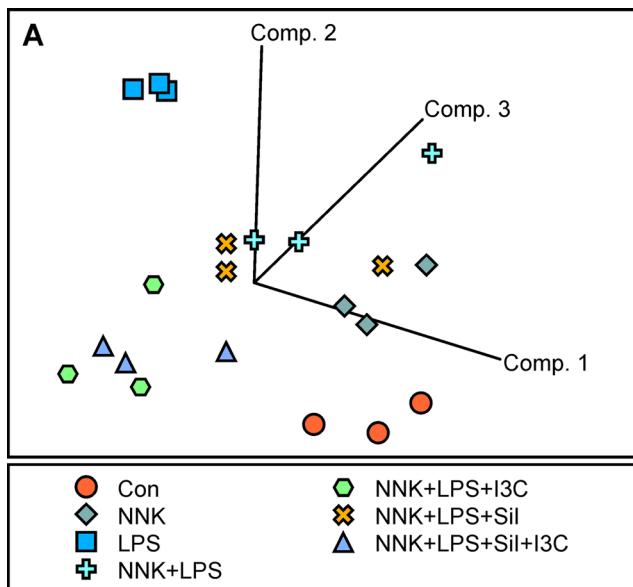


Table 2 Modulation of inflammation and immune response genes in normal lung tissues of LPS-treated mice and NNK- or NNK + LPS-induced mouse lung tumors

Inflammatory mediator gene	LPS vs control		NNK vs control		NNK + LPS vs control		Location	Type
	Fold change	FDR (<i>q</i> -value)	Fold change	FDR (<i>q</i> -value)	Fold change	FDR (<i>q</i> -value)		
<i>Ccl1</i>	36.205	1.53E-02					Extracellular space	Cytokine
<i>Ccl12</i>	25.125	8.08E-11					Extracellular space	Cytokine
<i>Ccl19</i>	91.648	4.48E-11			6.1	4.00E-02	Extracellular space	Cytokine
<i>Ccl2</i>	135.573	5.41E-13					Extracellular space	Cytokine
<i>Ccl20</i>	12.979	8.58E-09					Extracellular space	Cytokine
<i>Ccl27a</i>	-2.952	1.10E-02					Extracellular space	Cytokine
<i>Ccl3</i>	115.423	6.23E-53			2.9	1.00E-02	Extracellular space	Cytokine
<i>Ccl4</i>	377.494	4.78E-35			5.3	2.70E-03	Extracellular space	Cytokine
<i>Ccl5</i>	24.236	1.36E-27					Extracellular space	Cytokine
<i>Ccl7</i>	100.337	9.10E-13					Extracellular space	Cytokine
<i>Ccl8</i>	50.531	1.47E-18	3.731	2.42E-02	16.46	6.67E-10	Extracellular space	Other
<i>Ccl9</i>	6.46	5.75E-13					Extracellular space	Cytokine
<i>Cene1</i>	3.69	2.74E-09					Nucleus	Transcription regulator
<i>Cer1</i>	7.525	1.42E-19					Plasma membrane	G-protein coupled receptor
<i>Cer2</i>	2.553	1.92E-04					Plasma membrane	G-protein coupled receptor
<i>Cer4</i>	2.573	8.96E-03					Plasma membrane	G-protein coupled receptor
<i>Cer5</i>	16.82	6.83E-37			3.2	7.70E-07	Plasma membrane	G-protein coupled receptor
<i>Cer7</i>	2.717	1.81E-05					Plasma membrane	G-protein coupled receptor
<i>Cer8</i>	7.504	4.03E-06					Plasma membrane	G-protein coupled receptor
<i>Cer12</i>	4.436	2.11E-31					Plasma membrane	G-protein coupled receptor
<i>Cx3cr1</i>	2.918	2.28E-03					Plasma membrane	G-protein coupled receptor
<i>Cxcl1</i>	41.442	2.04E-08					Extracellular space	Cytokine
<i>Cxcl10</i>	360.764	2.97E-18			7.1	4.00E-03	Extracellular space	Cytokine
<i>Cxcl11</i>	913.572	2.30E-12					Extracellular space	Cytokine
<i>Cxcl13</i>	29.994	8.67E-10					Extracellular space	Cytokine
<i>Cxcl14</i>	2.133	7.43E-07					Extracellular space	Cytokine
<i>Cxcl16</i>	3.477	2.51E-36					Extracellular space	Cytokine
<i>Cxcl17</i>	2.552	1.16E-09					Other	Other
<i>Cxcl2</i>	149.94	3.67E-23					Extracellular space	Cytokine
<i>Cxcl3</i>	312.912	3.25E-14					Extracellular space	Cytokine
<i>Cxcl5</i>	46.061	2.15E-09					Extracellular space	Cytokine
<i>Cxcl9</i>	950.588	2.21E-25	8.168	2.10E-03	29.8	1.40E-08	Extracellular space	Cytokine
<i>Cxcr2</i>	12.68	8.78E-07	6.379	4.63E-03			Plasma membrane	G-protein coupled receptor

Table 2 continued

Inflammatory mediator gene	LPS vs control		NNK vs control		NNK + LPS vs control		Location	Type
	Fold change	FDR (<i>q</i> -value)	Fold change	FDR (<i>q</i> -value)	Fold change	FDR (<i>q</i> -value)		
<i>Cxcr3</i>	6.444	5.05E-09			4.4	3.00E-05	Plasma membrane	G-protein coupled receptor
<i>Cxcr5</i>	2.81	3.12E-02					Plasma membrane	G-protein coupled receptor
<i>Cxcr6</i>	21.303	3.06E-05			10.7	5.00E-03	Plasma membrane	G-protein coupled receptor
<i>Cxcr4</i>	-5.009	5.52E-04					Cytoplasm	Other
<i>Cd14</i>	19.79	2.70E-32					Plasma membrane	Transmembrane receptor
<i>Cd163</i>	-3.787	1.05E-04					Plasma membrane	Transmembrane receptor
<i>Cd163</i> molecule-like 1	3.864	3.39E-04					Plasma membrane	Other
<i>Cd177</i>	48.187	1.18E-11	4.664	4.16E-02			Cytoplasm	Other
<i>Cd180</i>	3.132	1.35E-03					Plasma membrane	Other
<i>Cd1d</i>	4.106	3.74E-09					Plasma membrane	Other
<i>Cd200r1</i>	3.038	3.81E-11					Plasma membrane	Other
<i>Cd200r4</i>	5.195	1.07E-20					Plasma membrane	Other
<i>Cd207</i>	-4.671	1.35E-07					Plasma membrane	Other
<i>Cd209a</i>	-8.38	1.47E-13					Plasma membrane	Other
<i>Cd209b</i>	-97.935	2.11E-13					Plasma membrane	Other
<i>Cd209c</i>	-11.457	2.19E-08					Plasma membrane	Other
<i>Cd209d</i>	-7.283	1.71E-04					Other	Other
<i>Cd209e</i>	-72.498	6.60E-04					Plasma membrane	Other
<i>Cd209f</i>	-5.547	2.54E-07					Other	Other
<i>Cd209 g</i>	-13.279	5.33E-06					Other	Other
<i>Cd226</i>	3.521	3.86E-05					Plasma membrane	Other
<i>Cd274</i>	15.854	1.15E-39					Plasma membrane	Enzyme
<i>Cd276</i>	2.657	1.08E-06					Plasma membrane	Other
<i>Cd28</i>	3.615	1.66E-05					Plasma membrane	Transmembrane receptor
<i>Cd300a</i>	3.632	1.76E-09					Plasma membrane	Transmembrane receptor
<i>Cd300 lb</i>	3.693	2.14E-06	2.704	1.27E-02			Plasma membrane	Other
<i>Cd300ld</i>	3.157	1.39E-04					Plasma membrane	Other
<i>Cd300lf</i>	5.306	3.76E-15					Plasma membrane	Other
<i>Cd300lg</i>	-3.816	1.49E-13					Other	Other
<i>Cd33</i>	4.432	1.19E-08	2.456	1.10E-02			Plasma membrane	Other
<i>Cd36</i>	-2.752	3.02E-14					Plasma membrane	Transmembrane receptor
<i>Cd37</i>	2.816	2.09E-04					Plasma membrane	Other
<i>Cd38</i>	2.11	1.75E-06					Plasma membrane	Enzyme

Table 2 continued

Inflammatory mediator gene	LPS vs control		NNK vs control		NNK + LPS vs control		Location	Type
	Fold change	FDR (<i>q</i> -value)	Fold change	FDR (<i>q</i> -value)	Fold change	FDR (<i>q</i> -value)		
<i>Cd3d</i>	4.467	2.31E-06					Plasma membrane	Transmembrane receptor
<i>Cd3e</i>	4.839	4.86E-07					Plasma membrane	Transmembrane receptor
<i>Cd3g</i>	5.331	5.35E-07					Plasma membrane	Transmembrane receptor
<i>Cd4</i>	3.359	3.70E-04					Plasma membrane	Transmembrane receptor
<i>Cd40</i>	3.058	1.18E-10					Plasma membrane	Transmembrane receptor
<i>Cd48</i>	3.082	3.08E-12					Plasma membrane	Other
<i>Cd5</i>	3.976	1.60E-05					Plasma membrane	Transmembrane receptor
<i>Cd52</i>	7.109	2.89E-15					Other	Other
<i>Cd53</i>	4.073	1.44E-20					Plasma membrane	Other
<i>Cd6</i>	4.314	1.90E-07					Plasma membrane	Transmembrane receptor
<i>Cd63</i>	2.818	8.36E-29					Plasma membrane	Other
<i>Cd68</i>	4.527	2.14E-36					Plasma membrane	Other
<i>Cd69</i>	7.603	1.42E-10					Plasma membrane	Transmembrane receptor
<i>Cd72</i>	4.553	9.85E-12					Plasma membrane	Transmembrane receptor
<i>Cd74</i>	4.519	7.84E-29	2.294	9.00E-08			Plasma membrane	Transmembrane receptor
	invariant chain							
<i>Cd80</i>	4.958	1.89E-14					Plasma membrane	Transmembrane receptor
<i>Cd83</i>	2.924	1.03E-06					Plasma membrane	Transmembrane receptor
<i>Cd84</i>	2.944	6.78E-14					Plasma membrane	Other
<i>Cd86</i>	6.086	1.26E-18					Plasma membrane	Transmembrane receptor
<i>Cd8a</i>	2.797	2.90E-02					Plasma membrane	Other
<i>Cd8b1</i>	2.387	2.70E-02					Plasma membrane	Other
<i>Cd96</i>	3.264	2.06E-03					Plasma membrane	Other
<i>Csf1</i>	3.527	3.05E-14					Extracellular space	Cytokine
<i>Csf2</i>	2.587	4.17E-05					Extracellular space	Cytokine
<i>Csf2ra</i>	3.561	2.54E-27					Plasma membrane	Transmembrane receptor
	(granulocyte-macrophage)							
<i>Csf2rb</i>	5.128	6.96E-19	2.188	8.21E-04			Plasma membrane	Transmembrane receptor
	(granulocyte-macrophage)							
<i>Csf3</i>	1794.345	1.30E-09					Extracellular space	Cytokine
<i>Csf3r</i>	12.544	2.54E-15	3.922	3.84E-04			Plasma membrane	Transmembrane receptor
<i>Ifng</i>	232.243	4.58E-13			18.4	4.40E-03	Extracellular space	Cytokine
<i>Ifngr2</i>	2.145	1.26E-12					Plasma membrane	Transmembrane receptor
<i>Il10</i>	15.933	1.23E-07					Extracellular space	Cytokine

Table 2 continued

Inflammatory mediator gene	LPS vs control		NNK vs control		NNK + LPS vs control		Location	Type
	Fold change	FDR (<i>q</i> -value)	Fold change	FDR (<i>q</i> -value)	Fold change	FDR (<i>q</i> -value)		
<i>Il10ra</i>	4.698	1.04E-13					Plasma membrane	Transmembrane receptor
<i>Il11</i>	4.122	5.63E-04					Extracellular space	Cytokine
<i>Il12a</i>	4.297	1.88E-09			-3.4	6.10E-04	Extracellular space	Cytokine
<i>Il12b</i>	7.052	8.07E-09					Extracellular space	Cytokine
<i>Il12rb1</i>	19.576	8.43E-11			4.3	1.00E-02	Plasma membrane	Transmembrane receptor
<i>Il13ra2</i>	8.786	3.78E-02					Plasma membrane	Transmembrane receptor
<i>Il15ra</i>	3.081	4.03E-14					Plasma membrane	Transmembrane receptor
<i>Il17a</i>	308.678	8.46E-10					Extracellular space	Cytokine
<i>Il17f</i>	12.583	6.20E-04					Extracellular space	Cytokine
<i>Il17ra</i>	2.457	5.57E-13					Plasma membrane	Transmembrane receptor
<i>Il17rd</i>	-2.29	2.93E-07					Cytoplasm	Other
<i>Il18 bp</i>	18.306	1.28E-29					Extracellular space	Other
<i>Il18rap</i>	7.726	5.10E-14	2.637	7.26E-03	2.5	4.20E-03	Plasma membrane	Transmembrane receptor
<i>Il1a</i>	17.081	1.55E-37					Extracellular space	Cytokine
<i>Il1b</i>	62.053	1.15E-51	2.892	1.57E-03			Extracellular space	Cytokine
<i>Il1f6</i>	78.035	4.82E-06					Extracellular space	Cytokine
<i>Il1f9</i>	110.662	1.94E-26	5.817	8.04E-04			Extracellular space	Cytokine
<i>Il1r2</i>	50.002	4.31E-10	12.312	6.92E-04			Plasma membrane	Transmembrane receptor
<i>Il1m</i>	47.07	9.78E-127					Extracellular space	Cytokine
<i>Il20rb</i>	3.352	1.75E-04			2.8	6.90E-03	Plasma membrane	Other
<i>Il21</i>	167.703	1.04E-08			35.6	3.00E-02	Extracellular space	Cytokine
<i>Il21r</i>	8.498	2.43E-09					Plasma membrane	Transmembrane receptor
<i>Il22</i>	32.108	3.37E-07					Extracellular space	Cytokine
<i>Il22ra2</i>	-3.902	1.90E-03					Plasma membrane	Transmembrane receptor
<i>Il23a</i>	12.471	1.16E-05					Extracellular space	Cytokine
<i>Il23r</i>	12.483	4.47E-08			8.2	7.60E-05	Plasma membrane	Transmembrane receptor
<i>Il24</i>	94.453	2.45E-06					Extracellular space	Cytokine
<i>Il27</i>	17.853	1.08E-18					Extracellular space	Cytokine
<i>Il27ra</i>	2.502	6.53E-05					Plasma membrane	Transmembrane receptor
<i>Il2ra</i>	6.388	1.86E-16			2.2	5.60E-03	Plasma membrane	Transmembrane receptor
<i>Il2rb</i>	10.454	6.53E-13			3	3.50E-03	Plasma membrane	Transmembrane receptor
<i>Il2rg</i>	3.421	7.39E-17					Plasma membrane	Transmembrane receptor
<i>Il4i1</i>	29.828	2.47E-21	2.69	4.81E-02			Cytoplasm	Enzyme

Table 2 continued

Inflammatory mediator gene	LPS vs control		NNK vs control		NNK + LPS vs control		Location	Type
	Fold change	FDR (<i>q</i> -value)	Fold change	FDR (<i>q</i> -value)	Fold change	FDR (<i>q</i> -value)		
<i>Il4ra</i>	2.183	1.72E-08					Plasma membrane	Transmembrane receptor
<i>Il5</i>	-8.302	4.79E-02					Extracellular space	Cytokine
<i>Il6</i>	160.774	2.99E-15					Extracellular space	Cytokine
<i>Il7r</i>	7.779	3.71E-18			3	3.10E-05	Plasma membrane	Transmembrane receptor
<i>Il9r</i>	-2.535	3.62E-02					Plasma membrane	Transmembrane receptor
<i>Tnf</i>	71.645	2.24E-20			3.3	3.00E-02	Extracellular space	Cytokine

responses were clearly more represented in lungs of mice treated with LPS than in mice treated with NNK + LPS (Fig. 1c, d). Table 2 shows common inflammatory and immune response genes differentially expressed in mice treated with LPS, NNK, and NNK + LPS. In mice treated with NNK + LPS, the proinflammatory genes *Ilg* and *Il21* were expressed at a high level (18-fold and 36-fold higher, respectively, compared to the level in the control group), although this level was much lower than that observed in the LPS group (increased by 232- and 168-fold, respectively). Contrary to inflammation and immunity-related genes, genes associated with calcium signaling, CDC42 signaling, allograft rejection, OX40 signaling, and B cell development were overrepresented in the NNK + LPS group compared to the LPS group. Mice treated with LPS exhibited underrepresentation of genes associated with cellular differentiation (Fig. 1d). Similar but relatively weaker effects were obtained in the NNK and NNK + LPS group.

Chemopreventive agents Sil and I3C reversed the expression of a subset of NNK + LPS-regulated genes

In this study, we sought to determine if the chemopreventive effects of Sil and I3C observed in the tumor bioassay would be paralleled by modulations in gene expression. Indeed, dietary administration of I3C + Sil or I3C alone to NNK + LPS-treated mice significantly reversed the expression of several chemokines, cytokines, putative oncogenes, and tumor suppressor genes to the level found in the vehicle control group. Genes whose expressions were altered in the NNK + LPS group by ≥ 5 -fold and modulated by I3C alone or Sil + I3C are listed in Table 3, whereas all the genes significantly altered in the NNK + LPS group and modulated by I3C alone or Sil + I3C are listed in Supplementary Table 5. Although Sil showed some modulatory activities, the effects were not significant. Hierarchical clustering of the genes deregulated by NNK + LPS and modulated by the chemopreventive agents indicated differential effects between Sil + I3C and I3C. For instance, a set genes downregulated by NNK + LPS group, compared to the vehicle group, were upregulated mainly by I3C (Fig. 2a, gray bar #1; Fig. 2b, gray bar #2). On the other hand, some genes whose expressions were upregulated by NNK + LPS were downregulated by both I3C and Sil + I3C (Fig. 2a, second cluster, black bar #2; Fig. 2b, first cluster black bar #1). Genes regulated by LPS were not affected significantly either by I3C or Sil + I3C (Fig. 2c). As shown earlier, tumor samples from animals treated with NNK + LPS displayed a set of 229 unique genes and the expression of these genes was reversed by both I3C and Sil + I3C (black

Table 3 Genes altered by NNK + LPS treatment by ≥ 5 -fold and modulated by I3C alone or Sil + I3C

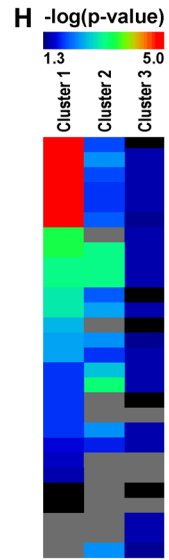
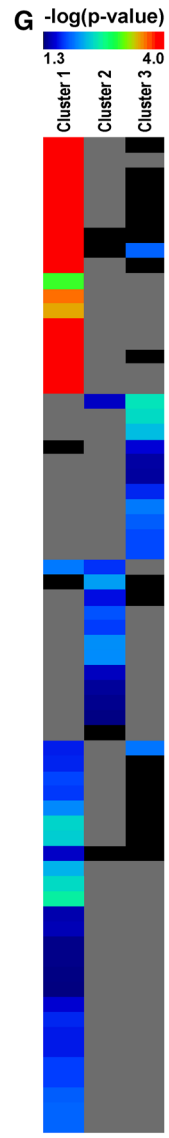
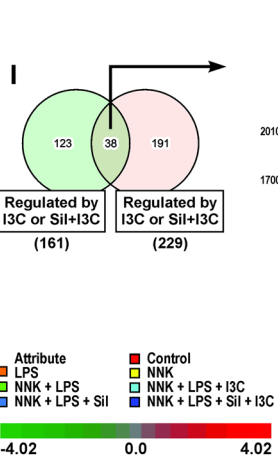
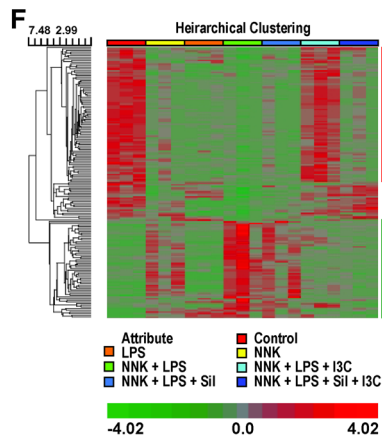
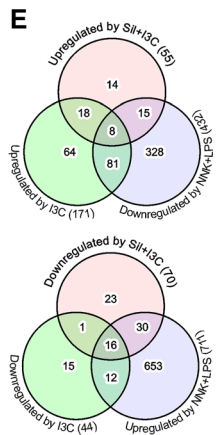
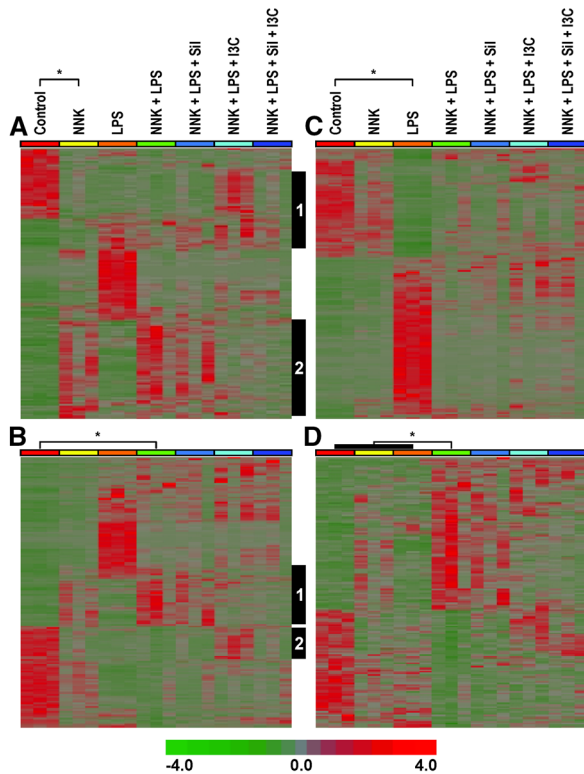
Gene	Description	Cellular location	Type(s)	NNK + LPS vs Con		NNK + LPS + Sil vs NNK + LPS		NNK + LPS + I3C vs NNK + LPS		NNK + LPS + Sil + I3C vs NNK + LPS	
				FC	FDR	FC	FDR	FC	FDR	FC	FDR
<i>Spag11b</i>	Sperm associated antigen 11B	Extracellular	Other	825.6	4.61E-16	-2	1	-9	1.40E-05	-12.3	5.70E-07
<i>Kng2</i>	Kinogen 1	Extracellular	Other	126.2	3.52E-05	1.4	1	-21.5	0.03	-8.3	0.31
<i>Cyp4a14</i>	Cytochrome P450, family 4, subfamily a, polypeptide 14	Cytoplasm	Enzyme	82.9	2.32E-05	-2.1	1	-15.6	0.0018	-28	0.00025
<i>Cyp2c40</i>	Cytochrome P450, family 2, subfamily c, polypeptide 40	Cytoplasm	Enzyme	56.4	0.00801	-1.2	1	-56.4	0.04	-19.1	0.05
<i>BC030867</i>	Chromosome 17 open reading frame 53	Other	Other	20.3	1.20E-10	-1.3	1	-4.7	0.0024	-6.2	0.00011
<i>Tmem213</i>	Transmembrane protein 213	Other	Other	14.1	4.49E-11	-1.3	1	-3.3	0.02	-2.7	0.13
<i>Necab1</i>	N-terminal EF-hand calcium binding protein 1	Cytoplasm	Other	13.3	0.00548	-2.5	1	-14	0.02	-19.7	0.0068
<i>Cyp4a12a</i>	Cytochrome P450, family 4, subfamily A, polypeptide 22	Cytoplasm	Enzyme	13.0	0.000312	-1.1	1	-3.2	0.38	-7.9	0.02
<i>Tnfrsf9</i>	Tumor necrosis factor (ligand) superfamily, member 9	Plasma membrane	Other	12.9	8.35E-14	-1.4	1	-2.8	0.02	-3.2	0.0068
<i>Gjb4</i>	Gap junction protein, beta 4, 30.3 kDa	Plasma membrane	Transporter	11.9	2.51E-11	-1.5	1	-2.7	0.02	-1.8	0.57
<i>Serpine1</i>	Serpin peptidase inhibitor, clade E, member 1	Extracellular	Other	9.7	0.000348	-1.7	1	-3	0.41	-6.7	0.03
<i>Areg</i>	Amphiregulin	Extracellular	Growth factor	8.4	1.58E-09	-1.9	1	-3.1	0.01	-2.5	0.14
<i>Ankrd22</i>	Ankyrin repeat domain 22	Nucleus	Transcription regulator	7.9	5.07E-05	-1.3	1	-2.2	0.28	-3.4	0.03
<i>Sprr1a</i>	Small proline-rich protein 1A	Plasma membrane	Other	7.5	0.0044	-1.7	1	-7.2	0.02	-2.5	0.96
<i>Ros1</i>	c-ros oncogene 1, receptor tyrosine kinase	Plasma membrane	Kinase	7.3	1.74E-11	-1.3	1	-1.7	0.53	-2.5	0.03
<i>Cxcr1</i>	Chemokine (C-X-C motif) receptor 1	Plasma membrane	G-protein coupled receptor	6.7	3.21E-07	-2.3	1	-4.9	0.00025	-4.6	0.00049
<i>Chdh</i>	Choline dehydrogenase	Cytoplasm	Enzyme	6.5	5.98E-05	-1.9	1	-3.6	0.05	-6	0.0012
<i>Fbp2</i>	Fructose-1,6-bisphosphatase 2	Cytoplasm	Phosphatase	6.4	3.02E-11	-1.3	1	-2.2	0.06	-2.4	0.03
<i>Myh13</i>	Myosin, heavy chain 13, skeletal muscle	Cytoplasm	Other	6.2	2.43E-10	-1.2	1	-2.8	0.0021	-3.6	2.30E-05
<i>Ivl</i>	Involucrin	Cytoplasm	Other	5.8	0.000146	-1.7	1	-3.8	0.03	-2.4	0.45
<i>Corin</i>	Corin, serine peptidase	Plasma membrane	Peptidase	5.3	9.56E-06	-1.4	1	-3	0.03	-2.9	0.05
<i>Arg2</i>	Arginase 2	Cytoplasm	Enzyme	5.2	4.71E-10	1	1	-1.5	0.89	-2.8	0.0014
<i>Yip7</i>	Yip1 domain family, member 7	Other	Other	-5.0	0.04	-1.3	1	6.2	0.02	1.2	1
<i>Rbm20</i>	RNA binding motif protein 20	Nucleus	Other	-5.1	7.45E-05	1.3	1	4.1	0.0061	1.5	1
<i>Obscn</i>	Obscurin, cytoskeletal calmodulin and titin-interacting RhoGEF	Cytoplasm	Kinase	-5.3	0.000984	1.2	1	4.8	0.01	1.4	1
<i>Lmod2</i>	Leiomodin 2 (cardiac)	Other	Other	-5.5	9.17E-09	1.2	1	3	0.0059	1.8	0.71
<i>Kcnj5</i>	Potassium inwardly rectifying channel, subfamily J, member 5	Plasma membrane	Ion channel	-5.6	1.72E-05	-1.2	1	4.4	0.0028	1.7	1

Table 3 continued

Gene	Description	Cellular location	Type(s)	NNK + LPS vs Con		NNK + LPS + SiI vs NNK + LPS		NNK + LPS + I3C vs NNK + LPS		NNK + LPS + SiI + I3C vs NNK + LPS	
				FC	FDR	FC	FDR	FC	FDR	FC	FDR
<i>Asgr1</i>	Asialoglycoprotein receptor 1	Plasma membrane	Transmembrane receptor	-5.7	3.66E-10	1.5	1	3.1	0.0018	4.2	4.20E-06
<i>Aqp7</i>	Aquaporin 7	Plasma membrane	Transporter	-6.0	0.01	1.6	1	7.6	0.0059	2.1	1
<i>Actn2</i>	Actinin, alpha 2	Nucleus	Transcription regulator	-6.2	0.00205	1.3	1	6.4	0.01	1.8	1
<i>Dusp27</i>	Dual specificity phosphatase 27 (putative)	Other	Phosphatase	-6.5	0.00344	1.9	1	6.2	0.02	2.1	1
<i>Tnni3</i>	Troponin I type 3 (cardiac)	Cytoplasm	Transporter	-6.8	5.40E-08	1.6	1	4.9	0.00014	2.3	0.28
<i>Tbx20</i>	T-box 20	Nucleus	Transcription regulator	-7.1	7.08E-05	-1	1	5.1	0.01	2.1	1
<i>Lrat</i>	Lecithin retinol acyltransferase (phosphatidylcholine-retinol O-acyltransferase)	Cytoplasm	Enzyme	-7.2	7.30E-12	-1.3	1	1.1	1	2.9	0.0052
<i>Casq2</i>	Calsequestrin 2 (cardiac muscle)	Cytoplasm	Other	-7.2	4.82E-06	1.3	1	5.2	0.0021	1.5	1
<i>Lrrc10</i>	Leucine rich repeat containing 10	Nucleus	Other	-7.3	0.02	2.3	1	11.1	0.0073	1.7	1
<i>Mybn</i>	Myopalladin	Cytoplasm	Other	-7.4	0.00471	1.7	1	7.2	0.02	2.6	1
<i>Tnn</i>	Titin	Cytoplasm	Kinase	-7.7	6.33E-06	1.5	1	5.1	0.0038	1.6	1
<i>Art1</i>	ADP-ribosyltransferase 1	Plasma membrane	Enzyme	-7.7	0.000363	1.1	1	5.6	0.02	1.7	1
<i>Slc22a1</i>	Solute carrier family 22 (organic cation transporter), member 1	Plasma membrane	Transporter	-7.7	0.000497	2.8	1	5.3	0.04	1.8	1
<i>Ebf2</i>	Early B-cell factor 2	Nucleus	Other	-7.9	0.02	2.2	1	15	0.00023	4.8	0.59
<i>Spon2</i>	Spondin 2, extracellular matrix protein	Extracellular	Other	-8.1	3.47E-11	1.3	1	1.2	1	3.6	0.0009
<i>Kcng2</i>	Potassium voltage-gated channel, subfamily G, member 2	Plasma membrane	Ion channel	-8.1	0.00194	3	1	7.9	0.0092	3.3	0.88
<i>Mlip</i>	Muscular LMNA-interacting protein	Nucleus	Other	-8.1	4.16E-05	-1.2	1	5.7	0.01	1.4	1
<i>Cypl1a1</i>	Cytochrome P450, family 1, subfamily A, polypeptide 1	Cytoplasm	Enzyme	-8.7	0.00279	1.3	1	85.7	9.00E-09	81.2	1.60E-08
<i>Myh4</i>	Myosin, light chain 4, alkali; atrial, embryonic	Cytoplasm	Other	-8.7	9.53E-07	1.4	1	6	0.00073	2.2	0.6
<i>Tnni2</i>	Troponin I type 2 (cardiac)	Cytoplasm	Other	-8.8	9.32E-06	1.7	1	7.4	0.00057	3	0.24
<i>Ctip2</i>	Cartilage intermediate layer protein 2	Extracellular	Other	-9.1	1.17E-05	2.4	1	5.8	0.01	1.5	1
<i>Hrc</i>	Histidine rich calcium binding protein	Cytoplasm	Other	-9.3	0.000604	1.9	1	5.9	0.04	1.8	1
<i>Csrp3</i>	Cysteine and glycine-rich protein 3 (cardiac LIM protein)	Nucleus	Other	-9.6	0.000885	1.4	1	6.9	0.03	2.6	0.97
<i>Myh7</i>	Myosin, light chain 7, regulatory	Cytoplasm	Enzyme	-9.8	2.76E-06	1.4	1	8	0.00026	3	0.25
<i>Eef1a2</i>	Eukaryotic translation elongation factor 1 alpha 2	Cytoplasm	Translation regulator	-10.0	0.00188	1.4	1	7.6	0.04	2.4	1

Table 3 continued

Gene	Description	Cellular location	Type(s)	NNK + LPS vs Con		NNK + LPS + Sil vs NNK + LPS		NNK + LPS + I3C vs NNK + LPS		NNK + LPS + Sil + I3C vs NNK + LPS	
				FC	FDR	FC	FDR	FC	FDR	FC	FDR
<i>Tnnc1</i>	Troponin C type 1 (slow)	Cytoplasm	Other	-10.7	3.61E-06	1.8	1	9.2	0.00019	3.7	0.15
<i>Ckm</i>	Creatine kinase, muscle	Cytoplasm	Kinase	-11.0	1.67E-05	1.7	1	6.9	0.0055	2.2	1
<i>Apobec2</i>	Apolipoprotein B mRNA editing enzyme, catalytic polypeptide-like 2	Other	Enzyme	-11.1	5.41E-05	3.1	1	10.6	0.0006	2.5	1
<i>Slc17a7</i>	Solute carrier family 17 (vesicular glutamate transporter), member 7	Plasma membrane	Transporter	-11.9	7.05E-09	2	1	7.1	0.00026	1.7	1
<i>Myh1</i>	Myosin, light chain 1, alkali; skeletal, fast	Cytoplasm	Other	-12.0	5.39E-07	1.7	1	5.3	0.02	1.3	1
<i>Lmod3</i>	Leiomodin 3 (fetal)	Other	Other	-12.2	0.00108	1.8	1	13.1	0.004	5.3	0.44
<i>Dhrs7c</i>	Dehydrogenase/reductase (SDR family) member 7C	Cytoplasm	Enzyme	-12.8	0.00147	1.2	1	8.8	0.05	3.1	1
<i>Myh3</i>	Myosin, light chain 3, alkali; ventricular, skeletal, slow	Cytoplasm	Other	-13.3	6.45E-07	-4.1	1	7.3	0.0074	2.5	1
<i>Mybphl</i>	Myosin binding protein H-like	Other	Other	-13.4	6.78E-05	2	1	9.5	0.0056	2.9	0.78
<i>Sln</i>	Sarcosin	Cytoplasm	Other	-13.8	0.000378	2.2	1	8.7	0.02	3	0.9
<i>Ckmt2</i>	Creatine kinase, mitochondrial 2 (sarcomeric)	Cytoplasm	Kinase	-14.6	5.78E-05	1.9	1	7.7	0.02	2.7	0.92
<i>Kenj3</i>	Potassium inwardly rectifying channel, subfamily J, member 3	Plasma membrane	Ion channel	-15.4	4.40E-10	1.3	1	11	1.60E-06	2.7	0.8
<i>Trims4</i>	Tripartite motif containing 54	Cytoplasm	Other	-18.5	2.69E-06	3.9	1	14.1	0.00019	4.6	0.39
<i>Nppa</i>	Natriuretic peptide A	Extracellular	Other	-18.6	5.39E-07	2.9	1	28.1	6.20E-08	1.2	1
<i>2310050B05Rik</i>				-23.3	2.18E-05	2.4	1	20.5	0.00057	5.8	0.86
<i>Hamp</i>	Hepcidin antimicrobial peptide	Extracellular	Other	-24.6	4.14E-05	1.7	1	21.6	0.00086	5.3	0.9
<i>Phn</i>	Phospholamban	Cytoplasm	Other	-34.9	1.09E-08	2.1	1	21.8	2.50E-05	4.7	0.35
<i>Slc28a1</i>	Solute carrier family 28 (concentrative nucleoside transporter), member 1	Plasma membrane	Transporter	-91.2	0.02	256.8	1	310.3	0.01	5.5	1



◀ **Fig. 2** Modulatory effects of Sil, I3C, and Sil + I3C on NNK + LPS-regulated genes. Unsupervised hierarchical clustering (euclidean distance matrix) of genes differentially expressed in (a) NNK vs. Con; (b) NNK + LPS vs. Con; and (c) LPS vs. Con. **d** Genes uniquely regulated by NNK + LPS vs. Con (not found in samples treated with NNK or LPS alone). *Gray vertical bars* show distinct clusters of differentially regulated genes being reversed by treatment with chemopreventive agents I3C or combination of Sil and I3C. **e** Venn diagram of genes regulated by NNK + LPS and reversed by I3C alone, Sil + I3C, or both I3C and Sil + I3C treatment. **f** Subset of genes regulated by NNK + LPS and modulated I3C alone and/or Sil + I3C. None of the genes were significantly modulated by Sil alone. **g** IPA canonical pathway analysis of the three clusters of genes shown in **f**. **h** Molecular and cellular functions from IPA of the three clusters of genes shown in **f**. **i** Venn diagram and Heatmap of genes uniquely regulated by NNK + LPS and modulation of the expression of these genes by I3C or Sil + I3C

bars #1 and #2, Fig. 2d). Supplementary Table S5 shows comparative modulatory effects of Sil, I3C, and Sil + I3C on genes whose levels were significantly altered by treatment with NNK + LPS.

Of the 432 genes downregulated by NNK + LPS, 81, 15, and 8 genes were upregulated by I3C alone, Sil + I3C, and by both I3C alone and Sil + I3C, respectively (Fig. 2e). Also, among genes that were upregulated in NNK + LPS group (711 genes), 12, 30, and 16 genes were downregulated by I3C alone, Sil + I3C, and 16 both I3C alone and Sil + I3C, respectively. The expression profiles of these differentially regulated genes were summarized in the hierarchical clustering heatmap with three visually distinct gene clusters (Fig. 2f, red and green bars). Gene enrichment analysis of the three main gene clusters showed that genes enriched in cluster 1 (downregulated by NNK + LPS, but upregulated by I3C) showed very strong association with calcium signaling, epithelial adherens junction signaling, actin cytoskeleton signaling, and RhoA signaling (Fig. 2g). The molecular and cellular function of these genes includes regulation of cell morphology, cellular assembly and organization, cellular development, cell survival, cell proliferation, and cell death (Fig. 2h). Genes in cluster 2 (genes downregulated by NNK + LPS, but upregulated only by Sil + I3C) were relatively fewer and had an association with AMPK signaling, G-alpha q signaling, calcium transport, and the visual cycle. These genes are involved in small molecule biochemistry, cell-to-cell signaling and interaction, molecular transport, and cell signaling and cell cycle. Genes in cluster 3 (upregulated by NNK + LPS, but downregulated by both I3C and Sil + I3C) showed association with circadian rhythm signaling, coagulation system, choline degradation, and arginase pathway (Fig. 2g) and are involved in protein processing, including protein synthesis, translational modification, and protein degradation. The genes from clusters 1, 2, and 3, their associated canonical pathways, and molecular and cellular functions are deposited at GEO

repository: <http://www.ncbi.nlm.nih.gov/geo/query/acc.cgi?acc=GSE64027>. Characterization of a subset of genes uniquely regulated in the NNK + LPS group identified 38 genes to be modulated by I3C or Sil + I3C (Fig. 2a, b). These genes were highly associated with cell signaling, lipid metabolism, and small molecule biochemistry (Fig. 2c).

Validation of RNA-seq results by qRT-PCR analysis

We selected 20 genes, based on their relevance to carcinogenesis and differential expression in RNA-Seq analysis, for verification by qRT-PCR. The qRT-PCR assays which were carried out on the same samples used for RNA-Seq analysis confirmed the sequencing results for all 20 genes. The results of 11 of these genes are shown in Fig. 3b. The magnitude of change in gene expression measured by RNA-Seq and qRT-PCR methods correlated well (Fig. 3a, b). In both assays, *Spag11b*, kininogen-2 (*Kn2*), neuropeptide Y receptor 2R (*Npy2r*), epiregulin (*Ereg*), retrotransposon-like 1 (*Rtl1*), c-ros oncogene 1 (*Ros1*), and claudin 2 (*Cldn2*) were overexpressed in the NNK + LPS group, as compared to the vehicle group, whereas aryl hydrocarbon receptor nuclear translocator-like (*Arntl*), neuronal PAS domain protein 2 (*Npas2*), early B-cell factor 2 (*Ebf2*), and cytochrome P450-1A1 (*Cyp1a1*) were downregulated in both RNA-Seq and qRT-PCR assays. The same trend was observed for the modulatory effects of the chemopreventive agents.

Discussion

Although epidemiological studies consistently demonstrated that smokers with COPD have a higher risk of lung cancer, compared to smokers without COPD [5, 6], the molecular links between the two diseases are not clear. Moreover, there are no safe and effective agents for the prevention of inflammation-related lung tumorigenesis. Therefore, in the present study, we sought to identify genes that are deregulated in lung tumors induced by NNK + LPS and to assess the efficacy of Sil and I3C, alone or in combination, to modulate the expression of these genes. In previous studies, we and others have shown that part of the chemopreventive activities of I3C and Sil are associated with suppression of inflammatory pathways [16, 20, 21].

Although mice treated with NNK + LPS were expected to exhibit the highest number of differentially regulated genes, the number of genes deregulated in this group was more than twofold lower than that of the LPS group. In addition, only 28 % of the genes differentially expressed in the LPS group were observed in the NNK + LPS group,

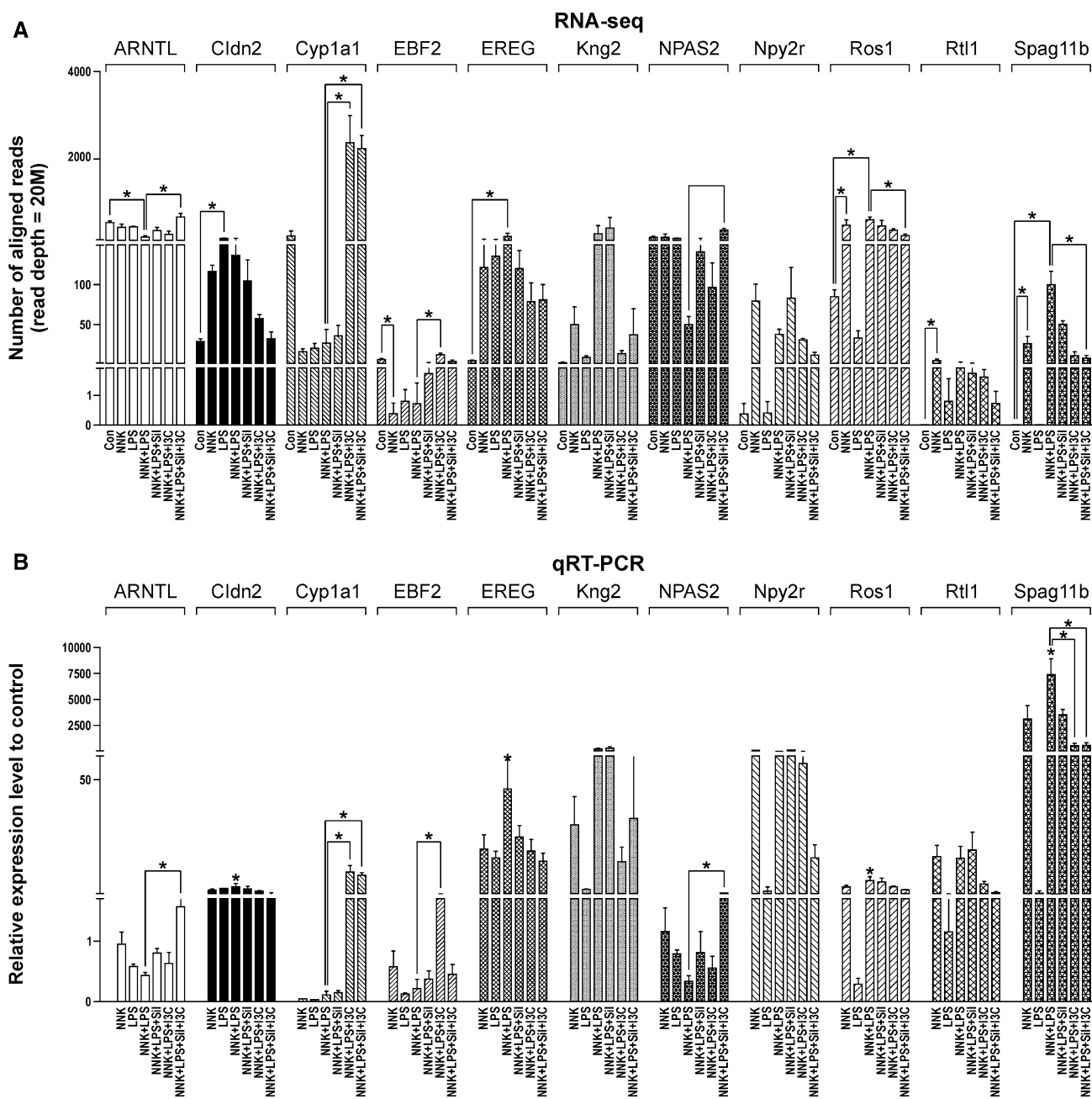


Fig. 3 Confirmation of RNA-Seq results (a) by qRT-PCR (b). RNA-Seq and QRT-PCR assays were performed as described in the “Materials and methods”. * $P < 0.05$

whereas 81 % of the genes deregulated in the NNK group were found in the NNK + LPS group. IPA results indicated that these differences were mainly due to the underrepresentation of inflammation and immune response genes in the NNK + LPS group. The low number of deregulated inflammation and immune response genes in the NNK + LPS group as compared to the LPS group could be ascribed partly to the comparison of tissues with different cellular constituents (tumors from the NNK + LPS group versus normal tissues from the LPS

group), and partly due to the defective expression of proinflammatory cytokines and chemokines by inflammatory cells associated with tumors. We found that levels of proinflammatory cytokines/chemokines such as *Tnf*, *Infg*, *IL21*, *Ccl4*, *Ccl8*, *Ccl19*, *Cxcl9*, and *Cxcl10* were at least tenfold lower in the NNK + LPS group as compared to the level in the LPS group, whereas a large number of proinflammatory genes were not deregulated at all in the NNK + LPS group (Table 1). This is typical of the situation seen in chronic inflammation-associated tumors in

which proinflammatory molecules are not expressed at adequate level to induce cytotoxic effects against tumor cells but are capable of inducing reactive oxygen/nitrogen species that cause DNA damage/mutation in the surrounding epithelial cells, predisposing them to premalignant transformation and tumor initiation [22]. Further growth of the premalignant cells could be supported by the proinflammatory and prosurvival signaling pathways NF- κ B and STAT3, which are activated by TNF alpha and IL-6, respectively. Low levels of cytokines have also been associated with poor antitumor immune response and tumor progression. Sustained low-level expression of interferon gamma has been found to promote the development of several types of tumors, including hepatoma, mammary adenocarcinoma, and melanoma, by upregulating genes involved in T cell immune tolerance such as *Pdl1*, *Pdl2*, *Ctla4*, and *Foxp3* [23]. In the present study, mice treated with NNK + LPS had 8- and 5-fold higher levels of *Pdl1* and *Foxp3*, respectively, as compared to the level in the control group (Supplementary Table S4), which suggests immune evasion of the lung tumor cells.

Some examples of individual cancer-associated genes that were significantly more up- or downregulated in the NNK + LPS group, compared to the NNK group, include the EGFR ligands *Ereg* and *Areg*, proto-oncogene tyrosine-protein kinase *Ros1*, and the putative tumor suppressor genes *Arntl* and *Npas2*. EREG and AREG (more than twofold higher expression in the NNK + LPS group compared to the NNK group) are cognate epidermal growth factor receptor ligands that have been shown to be overexpressed in most common human epithelial malignancies, including lung cancer [24, 25]. Observations made in different models of inflammation-related neoplasia suggest that *Ereg* and *Areg* are at the interface between inflammation and cancer since both genes are induced by inflammatory cytokines and overexpressed by tumor-associated cells such as fibroblasts and mast cells [26, 27]. *Ros1* receptor tyrosine kinase (overexpressed by sevenfold) has been found to be upregulated in 22 % of NSCLC and as an independent prognostic factor for overall survival of stage I lung adenocarcinoma patients [28]. The putative tumor suppressor genes *Arntl* and *Npas2* (underexpressed by 3- and 4-fold, respectively) are members of the circadian rhythm genes that maintain the timing for a range of physiological and behavioral processes. In addition to its tumor suppressor effects [29], ARNTL plays a role in the regulation of tobacco smoke-induced lung inflammatory responses since targeted deletion of the gene in the lung epithelium augmented cigarette smoke-induced pulmonary inflammation [30]. Also, human NPAS2 has a substantial impact on tumorigenesis, possibly through regulation of cancer-related genes, such as those involved in cell cycle checkpoint and DNA repair [31].

In mouse lung tumor bioassay, we observed that dietary administration of Sil + I3C to NNK + LPS-treated mice significantly reduced the tumor number as well as tumor size. To assess if the chemopreventive efficacy of Sil + I3C would be paralleled by modulation of NNK + LPS-induced gene alteration, we compared gene expression profiles of lung tumors from the control group versus groups treated with Sil, I3C, or Sil + I3C. Overall, dietary administration of Sil + I3C and I3C alone, but not Sil alone, reversed the expression of several cytokines, chemokines and putative oncogenes, and tumor suppressor genes to the level found in the vehicle control group (See Tables 2, 3). Since most of these genes have a well-established role in tumorigenesis, it is reasonable to postulate that modulation of the expression of these genes could be mechanistically related to the chemopreventive activities of Sil + I3C. Moreover, Sil + I3C and I3C alone modulated the expression of several cancer-related genes that were uniquely deregulated in mice treated with NNK + LPS. This group of genes includes *Hkdc1* [32], *Chdh* [33], *Rgs5* [34], *Filip1* [35], *Arntl* [29] and *Npas2* [31].

Among the genes whose expression was altered by the chemopreventive agents, the level of *Cyp1a1* was modulated to the greatest extent, being upregulated 86- and 81-fold by I3C and Sil + I3C, respectively. Although CYP1A1 converts some procarcinogens into ultimate carcinogens and thereby increasing the risk of DNA damage and tumorigenesis, it has also been reported to increase detoxication and clearance of NNK [36] and benzo(a)pyrene [37] and to convert 17 β -estradiol into 2-hydroxy-estradiol (2-OHE2), a potent cell cycle inhibitor, instead of 4-hydroxy-estradiol (4-OHE2), a highly DNA reactive metabolite [38]. In the present study, I3C was administered after treatment with NNK, and thus the chemopreventive activities of CYP1A1 cannot be attributed to modulation of carcinogen metabolism. However, since accumulating preclinical and clinical data show a strong link between estrogen and lung cancer development [39], CYP1A1 might suppress estrogen-related lung tumorigenesis by enhancing the preferential metabolism of estrogen toward the less toxic metabolite 2-hydroxy-estradiol.

Conclusions

Taken together, we showed that the expression of several cancer-associated genes was deregulated in inflammation-driven lung adenomas and these genes are potential targets for the chemopreventive activities of Sil + I3C. In particular, *Ereg*, *Areg*, *Ros1*, *Cyp1a1*, *Arntl*, and *Npas2* are interesting because of their established roles in

tumorigenesis. Currently, studies are underway to determine if similar gene expression alterations are found in inflammation-driven mouse lung adenocarcinomas and to assess the modulatory effects of Sil and I3C.

Acknowledgments This study was funded by a research grant to FK (CA-166,615-01). We want to express our indebtedness to Bob Carlson for his help in formatting the figures.

Conflict of interest The authors declare that they have no competing interests.

References

- Siegel R, Ma J, Zou Z, Jemal A. Cancer statistics. *CA Cancer J Clin.* 2014;64:9–29.
- Hecht SS. Lung carcinogenesis by tobacco smoke. *Int J Cancer.* 2012;131:2724–32.
- Thun MJ, Apicella LF, Henley SJ. Smoking vs other risk factors as the cause of smoking-attributable deaths: confounding in the courtroom. *JAMA.* 2000;284:706–12.
- Bach PB, Kattan MW, Thornquist MD, Kris MG, Tate RC, Barnett MJ, Hsieh LJ, Begg CB. Variations in lung cancer risk among smokers. *J Natl Cancer Inst.* 2003;95:470–8.
- Kiri VA, Soriano J, Visick G, Fabbri L. Recent trends in lung cancer and its association with COPD: an analysis using the UK GP Research Database. *Prim Care Respir J.* 2010;19:57–61.
- de Torres JP, Marín JM, Casanova C, Cote C, Carrizo S, Cordoba-Lanus E, Baz-Dávila R, Zulueta JJ, Aguirre-Jaime A, Saetta M, Cosío MG, Celli BR. Lung cancer in patients with chronic obstructive pulmonary disease—incidence and predicting factors. *Am J Respir Crit Care Med.* 2011;184:913–9.
- Pauly JL, Paszkiewicz G. Cigarette smoke, bacteria, mold, microbial toxins, and chronic lung inflammation. *J Oncol.* 2011;2011:8191291. doi:10.1155/2011/8191291.
- Hasday JD, Bascom R, Costa JJ, Fitzgerald T, Dubin W. Bacterial endotoxin is an active component of cigarette smoke. *Chest.* 1999;115:829–35.
- Larsson L, Pehrson C, Dechen T, Crane-Godreau M. Microbiological components in mainstream and sidestream cigarette smoke. *Tob Induc Dis.* 2012;10:13.
- Kharitonov SA, Sjöbring U. Lipopolysaccharide challenge of humans as a model for chronic obstructive lung disease exacerbations. *Contrib Microbiol.* 2007;14:83–100.
- Korsgren M, Linden M, Entwistle N, Cook J, Wollmer P, Andersson M, Larsson B, Greiff L. Inhalation of LPS induces inflammatory airway responses mimicking characteristics of chronic obstructive pulmonary disease. *Clin Physiol Funct Imag.* 2012;32:71–9.
- Melkamu T, Qian X, Upadhyaya P, O'Sullivan MG, Kassie F. Lipopolysaccharide enhances mouse lung tumorigenesis: a model for inflammation-driven lung cancer. *Vet Pathol.* 2013;50:895–902.
- Balkwill F, Mantovani A. Inflammation and cancer: back to Virchow? *Lancet.* 2001;357:539–45.
- Schetter AJ, Heegaard NH, Harris CC. Inflammation and cancer: interweaving microRNA, free radical, cytokine and p53 pathways. *Carcinogenesis.* 2010;31:37–49.
- Beane J, Vick J, Schembri F, Anderlind C, Gower A, Campbell J, Luo L, Zhang XH, Xiao J, Alekseyev YO, Wang S, Levy S, Massion PP, Lenburg M, Spira A. Characterizing the impact of smoking and lung cancer on the airway transcriptome using RNA-Seq. *Cancer Prev Res.* 2011;4:803–17.
- Dagne A, Melkamu T, Schutten MM, Qian X, Upadhyaya P, Luo X, Kassie F. Enhanced inhibition of lung adenocarcinoma by combinatorial treatment with indole-3-carbinol and silibinin in A/J mice. *Carcinogenesis.* 2011;32:561–7.
- Hecht SS, Lin D, Castonguay A. Effects of alpha-deuterium substitution on the mutagenicity of 4-(methyl-nitrosamino)-1-(3-pyridyl)-1-butanone (NNK). *Carcinogenesis.* 1983;4:305–10.
- Robinson MD, Smyth GK. Small-sample estimation of negative binomial dispersion, with applications to SAGE data. *Biostatistics.* 2008;9:321–32.
- Robinson MD, McCarthy DJ, Smyth GK, Edge R. A Bioconductor package for differential expression analysis of digital gene expression data. *Bioinformatics.* 2010;26:139–40.
- Aggarwal BB, Ichikawa H. Molecular targets and anticancer potential of indole-3-carbinol and its derivatives. *Cell Cycle.* 2005;4:1201–15.
- Agarwal R, Agarwal C, Ichikawa H, Singh RP, Aggarwal BB. Anticancer potential of silymarin: from bench to bed side. *Anticancer Res.* 2006;26:4457–98.
- Balkwill F, Charles KA, Mantovani A. Smoldering and polarized inflammation in the initiation and promotion of malignant disease. *Cancer Cell.* 2005;7:211–7.
- He YF, Wang XH, Zhang GM, Chen HT, Zhang H, Feng ZH. Sustained low-level expression of interferon-gamma promotes tumor development: potential insights in tumor prevention and tumor immunotherapy. *Cancer Immunol Immunother.* 2005;54:891–7.
- Zhang J, Iwanaga K, Choi KC, Wislez M, Raso MG, Wei W, Wistuba II, Kurie JM. Intratumoral epiregulin is a marker of advanced disease in non-small cell lung cancer patients and confers invasive properties on EGFR-mutant cells. *Cancer Prev Res.* 2008;1:201–7.
- Busser B, Sancey L, Brambilla E, Coll JL, Hurbin A. The multiple roles of amphiregulin in human cancer. *Biochim Biophys Acta.* 1816;201:119–31.
- Berasain C, Avila MA. Amphiregulin. *Sem Cell Dev Biol.* 2014;28:31–41.
- Neufert C, Becker C, Türeci Ö, Waldner MJ, Backert I, Floh K, Atreya I, Leppkes M, Jefremow A, Vieth M, Schneider-Stock R, Klingler P, Greten FR, Threadgill DW, Sahin U, Neurath MF. Tumor fibroblast—derived epiregulin promotes growth of colitis-associated neoplasms through ERK. *J Clin Invest.* 2013;123:1428–43.
- Lee HJ, Seol HS, Kim JY, Chun SM, Suh YA, Park YS, Kim SW, Choi CM, Park SI, Kim DK, Kim YH, Jang SI. ROS1 receptor tyrosine kinase, a druggable target, is frequently overexpressed in non-small cell lung carcinomas via genetic and epigenetic mechanisms. *Ann Surg Oncol.* 2013;20:200–8.
- Mullenders J, Fabius AW, Madiredjo M, Bernards R, Beijersbergen RL. A large scale shRNA barcode screen identifies the circadian clock component ARNTL as putative regulator of the p53 tumor suppressor pathway. *PLoS One.* 2009;4:e4798.
- Hwang JW, Sundar IK, Yao H, Sellix MT, Rahman I. Circadian clock function is disrupted by environmental tobacco/cigarette smoke, leading to lung inflammation and injury via a SIRT1-BMAL1 pathway. *FASEB J.* 2014;28:176–94.
- Hoffman AE, Zheng T, Ba Y, Zhu Y. The circadian gene NPAS2, a putative tumor suppressor, is involved in DNA damage response. *Mol Cancer Res.* 2008;6:1461–8.
- Li GH, Huang JF. Inferring therapeutic targets from heterogeneous data: HKDC1 is a novel potential therapeutic target for cancer. *Bioinformatics.* 2014;30:748–52.
- Wang Z, Dahiya S, Provencher H, Muir B, Carney E, Coser K, Shioda T, Ma XJ, Sgroi DC. The prognostic biomarkers HOXB13, IL17BR, and CHDH are regulated by estrogen in breast cancer. *Clin Cancer Res.* 2007;13:6327–34.

34. Silini A, Ghilardi C, Figini S, Sangalli F, Fruscio R, Dahse R, Pedley RB, Giavazzi R, Bani M. Regulator of G-protein signaling 5 (RGS5) protein: a novel marker of cancer vasculature elicited and sustained by the tumor's proangiogenic microenvironment. *Cell Mol Life Sci.* 2012;69:1167–78.
35. Kwon M, Hanna E, Lorang D, He M, Quick JS, Adem A, Stevenson C, Chung JY, Hewitt SW, Zudaire E, Esposito D, Cuttitta F, Libutti SK. Functional characterization of filamin a interacting protein 1-like, a novel candidate for antivasular cancer therapy. *Cancer Res.* 2008;68:7332–41.
36. Morse MA, LaGreca SD, Amin SG, Chung FL. Effects of indole-3-carbinol on lung tumorigenesis and DNA methylation induced by 4-(methylnitrosamino)-1-(3-pyridyl)-1-butanone (NNK) and on the metabolism and disposition of NNK in A/J mice. *Cancer Res.* 1990;50:2613–7.
37. Uno S, Dalton TP, Derkenne S, Curran CP, Miller ML, Shertzer HG, Nebert DW. Oral exposure to benzo[a]pyrene in the mouse: detoxication by inducible cytochrome P450 is more important than metabolic activation. *Mol Pharmacol.* 2004;5:1225–37.
38. Tsuchiya Y, Nakajima M, Yokoi T. Cytochrome P450-mediated metabolism of estrogens and its regulation in human. *Cancer Lett.* 2005;227:115–24.
39. Siegfried JM, Stabile LB. Estrogenic steroid hormones in lung cancer. *Semin Oncol.* 2014;41:5–16.